Quantum Distortion Gravity: Hidden Matter Sectors and the Fixed Point of the Einstein–Hilbert Flow

L. E. Pavesi*[1]

[1]Independent Researcher, Italy

October 12, 2026

Abstract

A first version of this work argued that asymptotic safety of Quantum Distortion Gravity (QDG) requires a sufficiently large hidden sector. That conclusion was drawn from a phenomenological one-loop flow whose gravitational functions are not derived from the Einstein–Hilbert action, and it does not survive a derivation from the Wetterich equation. We repeat the analysis with the flow derived in the Einstein–Hilbert truncation (optimised cutoff, harmonic gauge $\alpha = 1$, linear split, background S^4), with minimally coupled matter characterised by two integers (X, Y) that count scalars, Dirac fermions and vectors. Three results are obtained. (i) No hidden sector is needed for a non-Gaussian fixed point to exist: it exists for QDG-like content (n_f Dirac fermions and two Proca fields) for all $n_f < 10$, and for the full Standard-Model content, but for $n_f = 3$ and for the Standard Model it lies outside the range $g_* < 2$, $\lambda_* > -1$ in which the truncation is plausible. (ii) A hidden sector acts as a displacement in the (X, Y) plane: massless vectors, and for QDG-like content also scalars, move the fixed point back towards the pure-gravity one (one hidden vector suffices for $n_f = 3$; seven are needed for the Standard Model with the optimised cutoff), whereas hidden Dirac fermions move it away and, in the fermion-rich direction, destroy it by run-away. (iii) These statements depend on the scheme chosen for the matter cutoff; with a cutoff that is a function of $-\bar{D}^2$ only, the fermion and vector coefficients change and the fermion run-away is absent in the cases tested. The Weyl-gauged operators of QDG are not part of the flow, so none of this is a statement about the asymptotic safety of QDG itself.

Keywords: quantum gravity, metric-affine gravity, Weyl symmetry, asymptotic safety, functional renormalization group, fixed point, hidden sector, matter content

1 Introduction

Asymptotic safety [1] asks whether gravity has a non-Gaussian ultraviolet fixed point of the renormalization-group flow defined by the Wetterich equation [2]; evidence for such a fixed point in the Einstein–Hilbert (EH) truncation goes back to Reuter [3]. Quantum Distortion Gravity (QDG) [7] is a metric-affine theory with gauged Weyl symmetry which, in unitary gauge, reduces in the infrared to Einstein gravity coupled to two massive vector fields and matter. A natural question is whether the matter content of QDG, possibly supplemented by a hidden sector, supports a non-Gaussian fixed point.

A first version of the present work [9] answered that a fixed point exists only if a hidden sector with at least about four massless vector bosons is added to $n_f = 3$ Dirac fermions and the two QDG vectors. That answer was obtained with a one-loop system, used also in [8], in which the two gravitational functions $A(\lambda)$ and $B(\lambda)$ were taken to be mode-count expressions

*Corresponding author e-mail: lucapv02@gmail.com

of the volume term and were used as if they were the coefficient of the curvature term. The system is therefore a phenomenological *model*; in the pure-gravity limit it does not reproduce the Einstein–Hilbert fixed point (Section 6). The present paper replaces that analysis.

What is done. Section 2 recalls the EH flow derived from the Wetterich equation and its closed-form fixed point (a cubic equation), with minimally coupled matter described by two integers (X, Y). Section 3 applies it to QDG-like content without any hidden sector. Section 4 studies how hidden scalars, fermions and vectors displace the fixed point, for QDG-like content and for the Standard Model. Section 5 shows how the conclusions depend on the matter-cutoff scheme. Section 6 explains why the phenomenological flow of the first version gave a different answer, and Section 7 transcribes what is known from the R^2 truncation. Section 8 states what is and is not established.

Main results.

1. In the derived flow, a hidden sector is *not required* for the existence of the fixed point: it exists for QDG-like content for all $n_f < 10$ and for the Standard-Model content (Sections 3 and 4).

2. For these contents the fixed point lies outside the conventional range $g_* < 2$, $\lambda_* > -1$ (a convention, not a derived bound). Hidden massless vectors move it back inside, and the Standard-Model content needs seven of them with the optimised cutoff (Section 4).

3. The loss of the fixed point at $X = 14$ (equivalently at $n_f = 10$ for QDG-like content) is a property of fermion-rich contents with $Y < -6.17$ and of the matter-cutoff scheme used, not a general bound on matter (Sections 4 and 5).

Logical status. As in [7, 8], *Proposition* means proven within stated assumptions, *Remark* means not proven, *Open Problem* is a question we do not answer. Results are tagged `[DERIVED]` (derived in the paper or reproduced by the scripts accompanying it), `[INPUT]` (taken from the literature, not rederived), `[MODEL]` or `[OPEN]`. All numbers quoted are reproduced by the scripts listed in Appendix A.

2 The Einstein–Hilbert flow with minimally coupled matter

2.1 Truncation and inputs

We work in Euclidean signature on a background S^4 of radius r, $R = 12/r^2$, with the truncation

$$\Gamma_k[g, \bar{g}] = \frac{1}{16\pi G_k} \int d^4x\sqrt{g}\left(-R + 2\bar{\Lambda}_k\right) + \Gamma_k^{\rm gf} + \Gamma_k^{\rm gh} + \Gamma_k^{\rm matter}, \tag{1}$$

linear split $g = \bar{g} + h$ and harmonic gauge fixing with parameter $\alpha = 1$. Dimensionless couplings are $g = k^2 G_k$ and $\lambda = \bar{\Lambda}_k/k^2$; $\eta = \partial_t \ln G_k$, $t = \ln k$, so that $\beta_g = (2+\eta)g$. We use the optimised cutoff $R^{(0)}(z) = (1-z)\theta(1-z)$ for the gravitational sector.

Inputs `[INPUT]`. Three ingredients are taken from the literature and not rederived: the Hessian of the EH action on S^4 in harmonic gauge (Reuter [3]), in which the traceless modes $\hat{h}$ (9 components) and the trace φ (1 component) have operators $-\bar{D}^2 - 2\bar{\Lambda}_k + C\,R$ with $C = 2/3$ and $C = 0$, and the ghost operator is $-\bar{D}^2 - R/4$ (4 components); the heat-kernel coefficient $\frac{1}{6}R\,N$ for Bochner Laplacians on a bundle of fibre dimension N; and the threshold-function formalism. The remaining steps (trace, matching, closed form of the fixed point) are carried out here.

Gravitational flow `[DERIVED]`**.** Evaluating the Wetterich trace and matching the coefficients of $\sqrt{\bar{g}}\,R$ and $\sqrt{\bar{g}}$, with $u \equiv 1 - 2\lambda$,

$$\eta = \frac{g\,B_1(\lambda)}{1 - g\,B_2(\lambda)}, \qquad B_1 = \frac{1}{3\pi}\Big[\frac{5}{u} - \frac{9}{u^2} - 7\Big], \qquad B_2 = -\frac{1}{12\pi}\Big[\frac{5}{u} - \frac{6}{u^2}\Big], \tag{2}$$

$$\beta_\lambda = -(2-\eta)\lambda + \frac{g}{2\pi}\Big[\frac{5}{u} - 4 - \frac{5\eta}{6u}\Big]. \tag{3}$$

The coefficients B_1, B_2 and the volume term were checked against a numerical quadrature of the threshold functions to 10^{-9} at $\lambda = -0.3, 0, 0.1, 0.25$ (script `hs_checks.py`). The pure-gravity fixed point is

$$(g_*, \lambda_*) = (0.7073,\ 0.1932), \qquad \theta = 1.475 \pm 3.043\,i, \tag{4}$$

the standard optimised-cutoff result of the EH truncation (see e.g. [4]), where $\theta_i = -\mathrm{eig}(\partial\beta/\partial g_j)$. The anomalous dimension η is read off from the coefficient of R, not from the volume term.

Remark 2.1. The flow depends on the gauge ($\alpha = 1$ only), on the parametrisation of the metric (linear split), on the regulator and on the truncation. The fluctuations of the distortion tensor, of the Weyl gauge field V_μ, of the axial vector and of the dilaton are *not* in this flow. Whether they modify it is an open problem (Section 8).

2.2 Minimally coupled matter

Matter fields are minimally coupled to $g_{\mu\nu}$ with canonically normalised kinetic terms and no running of their wave-function renormalisation. Each field with fluctuation operator $\Delta = -\bar{D}^2 + E$ on a bundle of fibre dimension N contributes to $\partial_t\Gamma_k$ through $\mathrm{tr}\,b_2 = \frac{R}{6}N - \mathrm{tr}\,E$. With the matter cutoff taken to be a function of the whole operator Δ ("scheme B"; the gravitational cutoff is a function of $-\bar{D}^2$ only), only the threshold functions Φ^1_1, Φ^1_2 appear, and, normalising so that one real scalar has $X = Y = 1$,

$$\Delta\eta = \frac{g\,X}{6\pi}\,\Phi^1_1(0) = \frac{gX}{6\pi}, \qquad \Delta\beta_\lambda = \frac{g\,Y}{2\pi}\,\Phi^1_2(0) = \frac{gY}{4\pi} \qquad \text{(optimised cutoff)}. \tag{5}$$

The integers X, Y for a real scalar, a Dirac fermion (regulating the square of the Dirac operator, $(\gamma^\mu\bar{D}_\mu)^2 = -\bar{D}^2 + R/4$), a massless vector in Feynman gauge ($\Delta = -\bar{D}^2\delta^\mu{}_\nu + R^\mu{}_\nu$, plus two scalar ghosts) and a Proca field in the limit $m_V^2/k^2 \to 0$ (massless vector plus one scalar) are given in Table 1; they were recomputed by the script `hs_checks.py` from the heat-kernel counting. For N_S scalars, N_D Dirac fermions, N_V massless vectors and N_P Proca fields,

$$X = N_S + 2N_D - 4N_V - 3N_P, \qquad Y = N_S - 4N_D + 2N_V + 3N_P. \tag{6}$$

The coefficients of scheme B coincide with the combinations of N_S, N_D and N_V used in the

Table 1: Matter coefficients (scheme B). Scheme A is the cutoff that is a function of $-\bar{D}^2$ only (Section 5).

field	X (scheme B)	Y	X (scheme A)	remark
real scalar	$+1$	$+1$	$+1$	
Dirac fermion	$+2$	-4	-1	
massless vector	-4	$+2$	-1	with 2 ghosts
Proca ($m \to 0$)	-3	$+3$	0	assumption $m_V^2/k^2 \ll 1$

asymptotic-safety literature on matter content [5]; we have not compared them term by term with that reference. Two limitations should be kept in mind: the Proca entry is an assumption

on the value of the dimensionless mass at the fixed point and ignores non-minimal couplings of the vector to curvature, and *the values of X for fermions and vectors depend on the matter-cutoff scheme.*

For a hidden sector consisting of ΔN_S real scalars, ΔN_D Dirac fermions, ΔN_V massless vectors (for instance $\Delta N_V = \dim G_h$ for a hidden gauge group G_h, with the gauge couplings not run) and ΔN_P Proca fields, the content shifts as $(X, Y) \to (X, Y) + (\Delta X, \Delta Y)$ with $(\Delta X, \Delta Y)$ given by (6): a scalar moves the point by $(1, 1)$, a Dirac fermion by $(2, -4)$ and a massless vector by $(-4, 2)$.

2.3 Closed form of the fixed point

Collecting (2)–(5),

$$\eta = \frac{g\big[B_1(\lambda) + \frac{X}{6\pi}\big]}{1 - g\,B_2(\lambda)}, \qquad \beta_\lambda = -(2-\eta)\lambda + \frac{g}{2\pi}\Big[\frac{5}{u} - 4 - \frac{5\eta}{6u} + \frac{Y}{2}\Big]. \tag{7}$$

An *admissible* fixed point is a zero with $g_* > 0$, $\lambda_* < \frac{1}{2}$ (the pole of the threshold functions) and $1 - g_* B_2(\lambda_*) > 0$ (the same side of the pole of η as the Gaussian fixed point); where stated we add $\mathrm{Re}\,\theta_i > 0$ for both exponents.

Proposition 2.2 (Closed form `[DERIVED]`)**.** *The admissible fixed points of* (7) *are the points*

$$\lambda_* = \frac{1-u}{2}, \qquad g_* = \frac{2\pi}{N(u)}, \qquad N(u) = \frac{4}{u^2} - \frac{5}{2u} + \frac{c}{6}, \qquad c \equiv 14 - X, \tag{8}$$

where u is a root of

$$2c\,u^3 - (2c + 54 - 3Y)\,u^2 + 118\,u - 48 = 0 \tag{9}$$

with $u > 0$, $N(u) > 0$ and $N(u) - 2\pi B_2(u) = 3/u^2 - 5/(3u) + c/6 > 0$. There can be more than one such root.

Proof. At a fixed point with $g \neq 0$, $\beta_g = 0$ gives $\eta = -2$. Inserting $\eta = -2$ into (7), $g\,[B_1 + X/(6\pi) - 2B_2] = -2$. Since $-\pi B_1 = \frac{3}{u^2} - \frac{5}{3u} + \frac{7}{3}$ and $2\pi B_2 = \frac{1}{u^2} - \frac{5}{6u}$, this is $g = 2\pi/N(u)$ with N as in (8). With $\eta = -2$ the second condition reads $4\lambda = \frac{g}{2\pi}\big[\frac{20}{3u} - 4 + \frac{Y}{2}\big]$. Insert $g = 2\pi/N$, $\lambda = (1-u)/2$ and multiply by $6u^2$:

$$2(1-u)\big(24 - 15u + c\,u^2\big) = u\big(40 + (3Y - 24)u\big),$$

which expands to (9). Conversely, every root with $u > 0$ (i.e. $\lambda_* < \frac{1}{2}$), $N > 0$ (i.e. $g_* > 0$) and $1 - g_* B_2 = 1 - 2\pi B_2/N > 0$ gives a fixed point. The last condition is $N - 2\pi B_2 > 0$. □

For n_f Dirac fermions and two Proca fields, $X = 2n_f - 6$ and $Y = 6 - 4n_f$, and (9) becomes $(40 - 4n_f)u^3 - (76 + 8n_f)u^2 + 118u - 48 = 0$. For two massless vectors instead, $X = 2n_f - 8$, $Y = 4 - 4n_f$. Each root was inserted in the full flow (7): $|\beta_g|, |\beta_\lambda| < 10^{-13}$ and $\eta = -2.0000000000$ (script `hs_checks.py`). The critical exponents are obtained from the Jacobian by central differences.

Remark 2.3. The word "admissible" includes the condition $1 - g_* B_2 > 0$ only as a statement about the position of the fixed point relative to the pole of η; it does not prove that a flow trajectory connects the fixed point to the Gaussian one without crossing the pole.

3 QDG-like content without hidden sector

Table 2 gives the fixed point for n_f Dirac fermions and two Proca fields. Besides the exact optimised-cutoff fixed point, it reports a regulator-robust-existence (RRE) test: the fraction ρ_9 of nine regulators (optimised $R^{(0)} = a(1-z)\theta(1-z)$ with $a = 0.5, 0.75, 1, 1.5, 2, 3$ and exponential $R^{(0)} = a\,z/(e^z - 1)$ with $a = 0.5, 1, 2$) for which an admissible fixed point with $\mathrm{Re}\,\theta_i > 0$ exists, and whether for every regulator the fixed point closest to $\lambda = 0$ satisfies $g_* < 2$, $\lambda_* > -1$ ("in range"). This range is a convention to flag fixed points whose position makes the derivative expansion doubtful, not a derived bound.

Table 2: Fixed point of the derived flow, optimised cutoff ($a = 1$), for n_f Dirac fermions and two Proca fields (scheme B). ρ_9: fraction of the nine regulators with an admissible fixed point; "range": $g_* < 2$, $\lambda_* > -1$ for all nine. For $n_f = 10$ the exact optimised value has no fixed point while two of the nine regulators still have one.

n_f	X	Y	g_*	λ_*	θ_i	ρ_9	range
0	-6	6	0.5093	0.2290	$2.171 \pm 3.263\,i$	1	yes
1	-4	2	0.6204	0.2030	$1.760 \pm 3.023\,i$	1	yes
2	-2	-2	0.8362	0.1568	$1.226 \pm 2.531\,i$	1	yes
3	0	-6	2.7319	-0.3179	2.207, 0.723	1	no
4	2	-10	3.9037	-1.0676	3.161, 1.797	1	no
6	6	-18	5.9848	-2.8594	3.695, 2.146	1	no
8	10	-26	11.836	-7.8175	3.899, 2.249	1	no
9	12	-30	23.505	-17.597	3.957, 2.276	1	no
9.5	13	-32	46.841	-37.110	3.980, 2.286	0.78	no
10	14	-34	no admissible fixed point			0.22	–

The following facts are read from Table 2 and from the scripts (`hs_scan.py`).

1. The fixed point exists, with $\mathrm{Re}\,\theta_i > 0$ (smallest value 0.29), at every $n_f < 10$ tested (step 0.001). The branch is continuous in n_f; at $n_f = 0$ (two Proca fields only) it is a pure-gravity-like fixed point with a complex pair of exponents, λ_* changes sign at $n_f = 17/6$, and the exponents become two real numbers at $n_f \simeq 2.873$.

2. The denominator $1 - g_* B_2$ stays between 0.85 and 1.11 along the branch (step 0.01), so the pole of η is never approached.

3. At $n_f = 3$ the fixed point has $g_* = 2.73$, $\lambda_* = -0.318$ for the optimised cutoff and, over the nine regulators, $\max g_* = 2.83$ and $\min \lambda_* = -0.64$. It is therefore at the edge of the conventional range, and the truncation is not reliable there.

4. For $n_f \to 10^-$, $c = 14 - X = 2(10 - n_f) \to 0$ and one root of (9) escapes to infinity: $\lambda_*(10-n_f) \to -19.5$, $g_*(10-n_f) \to 52\pi/7 = 23.338$ (checked at $10-n_f = 10^{-1}, \ldots, 10^{-4}$). For two massless vectors in place of the Proca fields the limit is $n_f = 11$. For $n_f \in [10, 200)$ (step 0.01) the cubic has no admissible root for the Proca family.

Remark 3.1 (Meaning of n_{crit})**.** The value $n_f = 10$ is the point at which the fixed point runs off to $g_*, |\lambda_*| \to \infty$ along this family, *in scheme B and with the optimised cutoff*. Long before it the fixed point lies outside the range in which the truncation is plausible ($|\lambda_*| > 5$ for $n_f \gtrsim 7$). It should be read as an indicator of where the truncation stops being informative, not as a physical limit on the number of fermion species. The fixed-point existence is regulator-robust up to $n_f \simeq 9$ (Table 2).

Table 2 shows that for the physical fermion content $n_f = 3$ of the first version of this work an admissible fixed point *does* exist in the derived flow. The existence statement is conditional

on minimal coupling of the two Proca fields in the massless limit; this assumption is not tested here (Section 8).

4 Effect of a hidden sector

4.1 Geometry of the (X, Y) plane

The fixed point depends on the matter content only through (X, Y). Figure 1 shows the region in which an admissible fixed point exists (optimised cutoff, scheme B, $\mathrm{Re}\,\theta_i > 0$ not required), computed from (9). The following features follow from Proposition 2.2 and from a numerical scan.

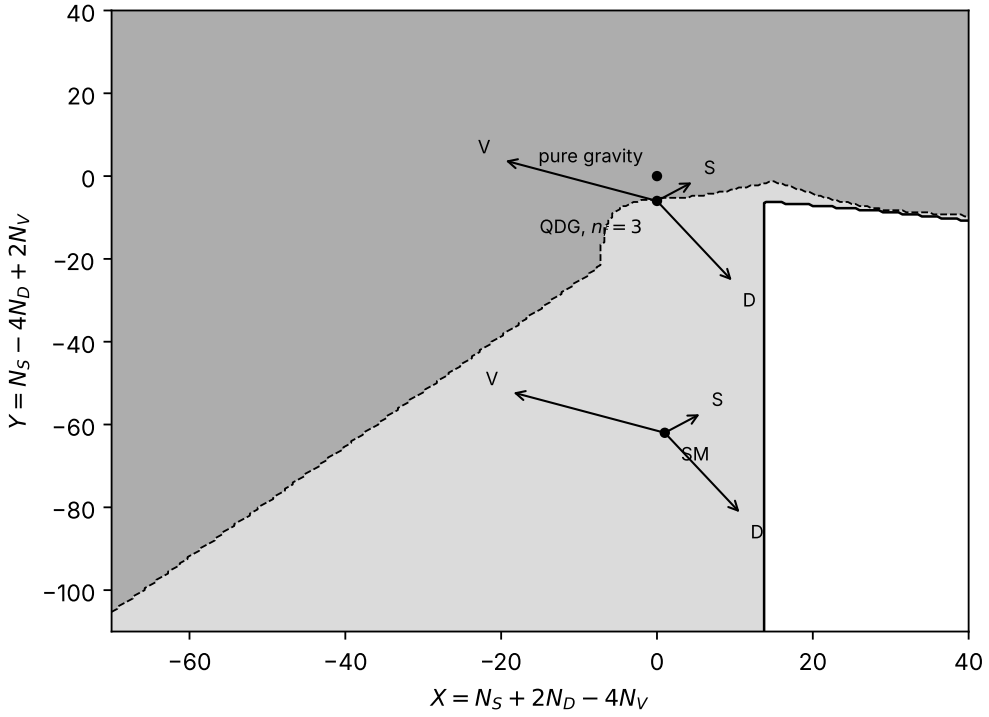


Figure 1: Existence of an admissible fixed point in the (X, Y) plane (optimised cutoff, scheme B). Light grey: fixed point exists but is outside the range $g_* < 2$, $\lambda_* > -1$; dark grey: exists and is inside that range; white: no admissible fixed point. Arrows: displacement by five hidden massless vectors (V), real scalars (S) or Dirac fermions (D), starting from QDG-like content with $n_f = 3$ and from the Standard Model. Script `hs_figure.py`.

1. For $c = 14 - X > 0$, i.e. $X < 14$, an admissible fixed point was found at every point tested (six values of $X < 14$, $Y \in [-5000, 5000]$; and along all rays of hidden vectors below, up to $\Delta N_V = 2000$).

2. For $Y < Y_0 = 18 - 118^2/576 = -6.17$ and $c \to 0^+$ the only admissible root escapes to infinity and there is none at $c = 0$ (the quadratic $(3Y - 54)u^2 + 118u - 48 = 0$ has negative discriminant); for $Y < -15.36$ there is none for any $X \geq 14$. For $Y > -6.17$ another root survives and the region extends beyond $X = 14$ up to a bounded value of X (about 277 at $Y = -6$ and 340 at $Y = 0$). These boundaries are numerical observations, not consequences of Proposition 2.2.

3. A fixed point near that boundary can have exponents with negative real part (for example $(X, Y) = (51, -12)$ has $\theta = (-148, -0.92)$); the notion of Section 3 with $\mathrm{Re}\,\theta_i > 0$ is stricter.

The loss of the fixed point at $X = 14$ therefore concerns contents that are fermion-rich ($Y = -4N_D + \cdots \ll 0$ while $X = 2N_D + \cdots > 14$); it is not a statement about matter in general. A hidden scalar moves a point along the diagonal $(1, 1)$, a hidden Dirac fermion along $(2, -4)$ and a hidden vector along $(-4, 2)$.

4.2 Hidden sector for QDG-like content with $n_f = 3$

Table 3 gives the effect of hidden sectors on the content $n_f = 3$ plus two Proca fields ($X = 0$, $Y = -6$). Rows with hidden gauge groups use $\Delta N_V = \dim G_h$ and Dirac fermions in the fundamental representation ($\Delta N_D = \dim R$ per flavour); gauge couplings of the hidden sector are not run.

Table 3: Hidden sector added to $n_f = 3$ Dirac fermions and two Proca fields (scheme B). Columns as in Table 2 (g_*, λ_*, θ_i: optimised cutoff; ρ_9 and "range": nine regulators). For one hidden real scalar the exponents are a complex pair with small real part (0.55; -0.09 for the exponential regulator $a = 0.5$), which is why $\rho_9 = 8/9$ and why "range" is "no" although the optimised-cutoff fixed point is inside the range.

hidden sector	X	Y	g_*	λ_*	θ_i	ρ_9	range
none	0	-6	2.7319	-0.3179	2.207, 0.723	1	no
1 massless vector	-4	-4	1.0629	0.0905	$1.080 \pm 1.762\,i$	1	yes
1 Proca field	-3	-3	0.9309	0.1297	$1.130 \pm 2.191\,i$	1	yes
$SU(2)_h$ (3 vectors)	-12	0	0.6884	0.1554	$1.678 \pm 2.242\,i$	1	yes
$SU(3)_h$ (8 vectors)	-32	10	0.4195	0.2059	$2.351 \pm 2.337\,i$	1	yes
1 real scalar	1	-5	1.4014	0.0596	$0.546 \pm 1.420\,i$	0.89	no
4 real scalars	4	-2	0.8352	0.1799	$1.068 \pm 3.016\,i$	1	yes
$SU(2)_h$ + 4 scalars	-8	4	0.5561	0.2108	$1.974 \pm 2.985\,i$	1	yes
$SU(3)_h$ + 1 flavour (8V, 3D)	-26	-2	0.6747	0.0776	$1.981 \pm 1.269\,i$	1	yes
$SU(3)_h$ + 3 flavours (8V, 9D)	-14	-26	1.4646	-0.8464	3.575, 1.866	1	no
1 Dirac fermion	2	-10	3.9037	-1.0676	3.161, 1.797	1	no
6 Dirac fermions	12	-30	23.505	-17.597	3.957, 2.276	1	no
7 Dirac fermions	14	-34	no admissible fixed point			0.22	–

1. **Vectors.** For $\Delta N_V \geq 1$ the fixed point exists and lies inside the conventional range; along the ray of hidden vectors g_* decreases and λ_* increases (Table 3, and $\Delta N_V = 12, 24, 48, 99$: $g_* = 0.33, 0.21, 0.126, 0.071$), and the exponents become a complex pair, as in pure gravity. With the optimised cutoff the range is entered for $\Delta N_V \simeq 0.19$ (the fixed point is a continuous function of the real parameter ΔN_V), so one hidden vector suffices. For two massless vectors in place of the two Proca fields the corresponding value is $\Delta N_V \simeq 0.50$.

2. **Scalars.** Hidden scalars also move the fixed point into the range ($\Delta N_S \simeq 0.56$), because Y rises faster than X (Figure 1). An admissible fixed point exists on the whole ray $\Delta N_S \in [0, 2000]$ (step 0.5).

3. **Dirac fermions.** Hidden fermions move the fixed point out of the range and to run-away: an admissible fixed point exists for $\Delta N_D \leq 6$ and not for $\Delta N_D \geq 7$ (total $n_f \geq 10$), which is the statement $n_{\mathrm{crit}} = 10$ of Section 3. With hidden gauge vectors the run-away is displaced: $SU(3)_h$ with three fundamental flavours ($\Delta N_V = 8$, $\Delta N_D = 9$) still has an admissible fixed point, but at $g_* = 1.46$, $\lambda_* = -0.85$ (the nine-regulator range test fails: $\max g_* = 2.01$, $\min \lambda_* = -2.70$).

4.3 Hidden sector for the Standard-Model content

For the Standard Model with minimally coupled fields ($N_S = 4$, $N_D = 22.5$, $N_V = 12$; 22.5 is 15 Weyl fermions $\times$ 3 generations counted as Dirac) the fixed point exists and is regulator-robust ($\rho_9 = 1$), at $(g_*, \lambda_*) = (3.217, -4.393)$, $\theta = (3.926, 2.083)$ for the optimised cutoff; over the nine regulators the extreme values are $g_* = 4.32$ and $\lambda_* = -13.8$. It is at extreme couplings. With four generations ($N_D = 30$, $X = 16$, $Y = -92$) there is no fixed point for any of the nine regulators.

Table 4: Hidden sector added to the Standard-Model content ($X = 1$, $Y = -62$), scheme B. "range": $g_* < 2$, $\lambda_* > -1$ for the optimised cutoff alone ("9 reg.": for all nine regulators).

hidden sector	X	Y	g_*	λ_*	ρ_9	range	9 reg.
none	1	−62	3.217	−4.393	1	no	no
1 massless vector	−3	−60	2.445	−3.221	1	no	no
$SU(2)_h$ (3 vectors)	−11	−56	1.642	−2.004	1	no	no
$SU(3)_h$ (8 vectors)	−31	−46	0.882	−0.862	1	yes	no
12 vectors	−47	−38	0.633	−0.495	1	yes	no
24 vectors	−95	−14	0.329	−0.067	1	yes	yes
1 real scalar	2	−61	3.497	−4.711	1	no	no
8 real scalars	9	−54	8.627	−10.538	1	no	no
13 real scalars	14	−49	none (Litim $a = 1$)		0.22	–	–
1 Dirac fermion	3	−66	3.801	−5.512	1	no	no
5 Dirac fermions	11	−82	13.896	−24.807	1	no	no
4 generations	16	−92	none		0	–	–
4 gen. + 1 vector	12	−90	20.715	−40.320	0.78	no	no
4 gen. + 2 vectors	8	−88	6.880	−13.072	1	no	no
4 gen. + 4 vectors	0	−84	2.926	−5.289	1	no	no
4 gen. + 24 vectors	−80	−44	0.404	−0.355	1	yes	no

Table 4 shows the same pattern. Hidden vectors improve the position monotonically; with the optimised cutoff $\lambda_* = -1$ is reached at exactly $\Delta N_V = 7$ ($u = 3$ in (9) gives $198\,\Delta N_V - 1206 = 180$), so $SU(3)_h$ (eight vectors) is the smallest simple hidden gauge group that brings the optimised-cutoff fixed point into the range, while the nine-regulator test is satisfied only for much larger numbers (it fails for 12 vectors, where $\min \lambda_* = -1.64$, and holds for 24). Hidden scalars and fermions move it outward, and thirteen hidden scalars ($X = 14$) destroy it for the optimised cutoff. A single hidden vector suffices to restore existence for the four-generation Standard Model ($X = 16 \to 12 < 14$), but the resulting fixed point is far outside the range, with $g_* = 20.7$ for one vector.

4.4 Summary of the displacement picture

Remark 4.1 (Summary `[DERIVED, numerical]`)**.** In the derived EH flow (scheme B, optimised cutoff, minimal coupling), for the contents $n_f = 3$ with two Proca fields and for the Standard Model: (a) a non-Gaussian fixed point exists without any hidden sector; (b) it exists for every number of hidden massless vectors tested ($\Delta N_V \leq 2000$) and moves towards the pure-gravity fixed point as ΔN_V grows; (c) hidden Dirac fermions move it outward and eliminate it at $X = 14$, i.e. at $\Delta N_D = 7$ for $n_f = 3$; (d) hidden scalars move it inward for $n_f = 3$ (and the fixed point is lost only for $X \geq 14$ with $Y < Y_{\min}(X)$), but outward for the Standard Model, where $\Delta N_S = 13$ eliminates it.

It is an observation on the cubic (9): existence on the rays was verified numerically, not proven. Item (d) shows that "extra fields destroy the fixed point" is true only along directions that approach the boundary $X = 14$ from a fermion-rich base.

5 Dependence on the matter-cutoff scheme

The gravitational cutoff of Section 2 is a function of $-\bar{D}^2$ only (type A), with the curvature terms of the Hessian expanded in the propagator. For matter we used a cutoff that is a function of the whole operator $-\bar{D}^2 + E$ (type B). If instead the matter cutoff is also a function of $-\bar{D}^2$ only, the same heat-kernel counting gives, for the optimised cutoff ($\Phi^2_2(0)/\Phi^1_1(0) = \frac{1}{2}$), $X = \sum 12\, n_w\, (\frac{N}{6} - \frac{1}{2}\,\mathrm{tr}E/R)$ instead of $12\, n_w(\frac{N}{6} - \mathrm{tr}E/R)$, with Y unchanged. This gives $X_D = -1$ and $X_V = -1$ (Table 1), so that $X = N_S - N_D - N_V$ (Proca fields count 0). We call this scheme A.

Table 5: Scheme A (matter cutoff a function of $-\bar{D}^2$ only), optimised cutoff $a = 1$. Only the optimised cutoff was computed; the nine-regulator test was not repeated in this scheme.

content	X	Y	g_*	λ_*	θ_i
$n_f = 0$, 2 Proca	0	6	0.5103	0.2399	$2.227 \pm 3.595\, i$
$n_f = 3$, 2 Proca	-3	-6	1.8188	-0.1132	1.491, 0.978
$n_f = 6$, 2 Proca	-6	-18	2.1294	-0.8997	3.430, 1.826
$n_f = 10$, 2 Proca	-10	-34	1.7379	-1.3259	3.722, 1.955
$n_f = 50$, 2 Proca	-50	-194	0.6068	-2.4107	3.962, 2.009
$n_f = 1000$, 2 Proca	-1000	-3994	0.0372	-2.9635	3.998, 2.001
Standard Model	-30.5	-62	0.8942	-1.1744	3.831, 1.962
$n_f = 3 + 1$ hidden vector	-4	-4	1.0629	0.0905	$1.080 \pm 1.762\, i$
$n_f = 3 + 8$ hidden vectors	-11	10	0.4370	0.2423	$2.471 \pm 3.261\, i$

Table 5 shows three differences. (i) The fermion run-away is absent: fixed points exist for all n_f tested up to 1000, because X decreases with n_f and stays below 14 (we found admissible roots at all of 6×2001 points with $X < 14$ and $Y \in [-5000, 5000]$). (ii) At $n_f = 3$ the fixed point is inside the range, $(g_*, \lambda_*) = (1.82, -0.11)$, instead of at its edge. (iii) The Standard-Model fixed point moves to $(0.894, -1.174)$, just outside the range in λ_*. Hidden vectors move the fixed point inward in both schemes (the entries for one hidden vector coincide because $(X, Y) = (-4, -4)$ in both).

Remark 5.1. We do not know which scheme corresponds to the matter literature [5]; the abstract of that work states that, within certain approximations, there is a maximal number of scalar and fermion degrees of freedom compatible with an interacting fixed point for a given number of gauge fields. Our scheme-A result for this content shows no such bound among the cases tested. We do not claim that this contradicts that work, whose truncation, gauge and counting may differ. The point is that the existence boundary $X = 14$, $n_{\mathrm{crit}} = 10$ and every statement that fermions *destroy* the fixed point are statements about scheme B.

6 Relation to the phenomenological model flow

The first version of this work and the companion analysis [8] used the one-loop *model*

$$\eta = -\frac{g\, A(\lambda)}{1 - g\, B(\lambda)} + C_\eta g, \qquad \beta_\lambda = -(2-\eta)\lambda + \frac{g}{2\pi} B(\lambda) + C_{\mathrm{bl}}\, g + \frac{72\lambda^2}{16\pi^2}, \tag{10}$$

with $A(\lambda) = \frac{5}{1-2\lambda} - \frac{3}{1-\lambda} - 1$, $B = A + 1$ and $C_\eta = (n_f - 4)/(3\pi)$. The functions A, B have the form of signed multiplicities of the volume term and are used as the coefficient of R; the term $72\lambda^2/16\pi^2$ is not derived from the action. The model is not the EH flow: its pure-gravity fixed point is $(0.350, 0.031)$ instead of (4), it has a pole at $\lambda = 1$ that the derived flow does not have, and no rescaling of g or λ maps one onto the other. We label it `[MODEL]`.

Reproduction of the first version. The first version used $C_{\rm bl} = 2(1 - n_f)/\pi$ and shifted only C_η by $-2n_{\rm hidden}/(3\pi)$ for a hidden sector. With these coefficients the scripts reproduce the table of [8] for $n_f = 0, 1, 2$, e.g. $(g_*, \lambda_*) = (0.4727, -0.0425)$, $\theta = (8.855, 3.463)$ at $n_f = 2$, no fixed point at $n_f = 3$, and the hidden-sector values $(11.09, -2.71)$ for four extra vectors and $(5.13, -1.40)$ for eight (script `hs_model.py`). The numbers of the first version are therefore internally reproducible.

The result depends on the coefficient $C_{\rm bl}$. The volume coefficient of the matter contribution follows from the heat-kernel counting, $\Delta\beta_\lambda = gY/(4\pi)$, i.e. $-1/\pi$ per Dirac fermion; the coefficient used in the first version is $-2/\pi$ per Dirac fermion, twice as large, and it does not follow from any consistent counting. With the counting-consistent coefficient $C_{\rm bl} = (3 - 2n_f)/(2\pi)$ (two Proca fields) the model has, at $n_f = 3$, the fixed point

$$(g_*, \lambda_*) = (0.4318,\ -0.0194), \qquad \theta = (9.446,\ 3.519), \tag{11}$$

and the fixed point disappears at $n_f = 4.8966$, where $1 - g_* B \to 0$. At fixed $C_\eta = -1/(3\pi)$ the fixed point exists for $C_{\rm bl} \gtrsim -1.08$; the first version's value at $n_f = 3$ is -1.273, below this threshold, and the counting-consistent value is -0.477, above it. Hidden massless vectors added consistently ($C_\eta \to C_\eta - 2/(3\pi)$ and $C_{\rm bl} \to C_{\rm bl} + 1/(2\pi)$ per vector) give $(g_*, \lambda_*) = (0.395, 0.000)$, $(0.341, 0.030)$, $(0.262, 0.081)$ for $1, 3, 8$ vectors: the model also has a fixed point without a hidden sector, and hidden vectors move it towards the origin, as in the derived flow. The claim that a hidden sector is *required* was an effect of the factor in $C_{\rm bl}$, not a property of the model or of QDG.

7 The higher-derivative truncation

The extension of the truncation by an R^2 term was studied by Lauscher and Reuter [6]. In the regulator scans transcribed from the output files of the book's scripts (which require the package `sympy`, unavailable here; *the numbers below were not recomputed for this paper*), with the exponential family $R^{(0)}(y) = s\, y/(e^{sy} - 1)$ and $s \in \{1, \ldots, 2.5\}$ sampled, the pure-gravity fixed point persists with three relevant directions and a complex pair of exponents, and for Standard-Model matter ($N_S = 4$, $N_D = 22.5$, $N_V = 12$) the fixed point exists with real positive exponents (e.g. $\theta = \{15.32, 3.64, 1.90\}$ at $s = 1.5$) down to a saddle–node at $s_{\rm fold} = 1.0721$ ($N_D = 22.5$, converged for $N_G \geq 480$), after which the branch with three relevant directions ends; $s_{\rm fold} = 1.0310$ for $N_D = 15$; for $N_D = 27$ there is no fold and the branch runs away at $s \gtrsim 1.083$; at fixed $s = 2$ the fixed point is followed up to $N_D = 28$ and is lost at $N_D = 28.5$. Earlier "edges" defined by a diverging leading exponent (1.0344, 1.0722) were artefacts of the finite-difference step and are withdrawn. None of these values is an absence proof, and no existence threshold in s is claimed. The matter coefficients in the R^2 sector are valid only for one projection and the same gauge $\alpha = 1$ is used.

These results concern minimally coupled matter without a hidden sector. A parametric estimate of the size of R^2 terms (of order $g_*/16\pi^2$) is not a substitute for the flow in the enlarged truncation, and we make no statement on the effect of a hidden sector in that truncation (Open Problem 8.4).

8 Discussion

8.1 What is and is not established

8.2 Limitations

1. The flow is the EH flow with minimally coupled matter. The Weyl gauge field V_μ, the axial vector $\tilde{a}_\mu$, the dilaton and the non-minimal couplings of QDG are not in it; in unitary

Table 6: Status of the results of this paper.

Result	Status	Condition / comment
EH flow, closed-form fixed point (cubic)	DERIVED	Hessian constants of Reuter: input; gauge $\alpha = 1$, linear split, optimised cutoff
X, Y counting of scalars, Dirac fermions, vectors	DERIVED	Scheme B; Proca = vector + scalar is an assumption
Fixed point exists for $n_f < 10$ (QDG-like) and for the SM	DERIVED (numerical for regulators)	Minimal coupling; scheme B
Hidden vectors move the fixed point inward	DERIVED (numerical)	Both schemes; rays tested to $\Delta N_V = 2000$
Hidden fermions destroy the fixed point at $X = 14$	DERIVED	Scheme B only; absent in scheme A (cases tested)
Hidden sector *required* for existence	NOT SUPPORTED	Result of a model coefficient
Phenomenological model flow	MODEL	Not the EH flow
R^2 truncation results	TRANSCRIBED	Not recomputed here
Weyl-gauged QDG sector in the flow	OPEN	Not included
Gauge and parametrisation dependence	OPEN	Not varied

gauge the two QDG vectors are treated as Proca fields in the limit $m_V^2/k^2 \to 0$, which is an assumption. Whether the QDG-specific operators modify η and β_λ is open, in particular whether the functions A, B of the model could be obtained from them.

2. Gauge ($\alpha = 1$), parametrisation (linear split) and regulator dependence: only the regulator was varied, over nine profiles. The location of the fixed point and the exponents depend on all three.

3. Fixed points that matter here ($n_f = 3$, the Standard Model) are at $g_* \gtrsim 2.7$, $|\lambda_*|$ up to several units, outside the range in which the expansion in R/k^2 can be trusted; the range itself is a convention.

4. The matter-cutoff scheme changes X for fermions and vectors (Section 5); the scheme of the literature has not been identified.

5. Hidden sectors are assumed to be coupled only gravitationally in the flow (hidden gauge and Yukawa couplings are not run), and no phenomenological constraint on a hidden sector (for instance on extra radiation) has been examined.

6. The Coleman–Weinberg generation of an infrared scale with a second Weyl scalar, discussed in the first version, is not retained: it is logically independent of the fixed-point question, a second scalar σ is not part of the QDG field content, and the status of ϕ_0 as a physical parameter in a Weyl-gauged theory (where it is a gauge choice in unitary gauge) is doubtful. We make no statement on scale generation.

8.3 Open problems

Open Problem 8.1. Compute the contributions of V_μ, $\tilde{a}_\mu$ and the dilaton, with their non-minimal couplings to curvature, to η and β_λ and compare with the counting (X, Y) of Table 1.

Open Problem 8.2. Repeat the derivation for $\alpha \neq 1$ (including $\alpha \to 0$) and for the exponential parametrisation of the metric, and determine which results of Sections 3–5 survive.

Open Problem 8.3. Identify the matter-cutoff scheme for which X is regulator-independent in the sense of the matter literature, and repeat Section 4 in that scheme.

Open Problem 8.4. Extend the hidden-sector analysis to the R^2 truncation and beyond ($R^2_{\mu\nu}$, Weyl-squared), and decide whether a hidden sector changes the number of relevant directions.

Open Problem 8.5. Compute $X_P(w_V)$ and $Y_P(w_V)$ for finite $w_V = m_V^2/k^2$ and the contribution of non-minimal couplings of the vector to curvature.

9 Conclusions

Within the Einstein–Hilbert truncation derived from the Wetterich equation, with minimally coupled matter in harmonic gauge and with the optimised cutoff, a non-Gaussian fixed point exists for the QDG-like content ($n_f < 10$ Dirac fermions and two Proca fields) and for the Standard-Model content without any hidden sector. The claim that asymptotic safety *requires* a sufficiently large hidden sector is not supported: it rested on a phenomenological flow and on a coefficient in β_λ that does not follow from the heat-kernel counting. What a hidden sector does is displace the content in the (X, Y) plane: massless vectors (and, for $n_f = 3$, scalars) move the fixed point back towards the pure-gravity one, into the range where the truncation is plausible, while Dirac fermions move it out and, in the optimised-cutoff scheme B, remove it at $X = 14$. All of this is conditional on minimal coupling, on the matter-cutoff scheme and on the gauge, and none of it is a statement about the Weyl-gauged operators of QDG, which remain outside the flow.

Acknowledgements. The author thanks the scientific community for discussions and feedback. This work was conducted without institutional or financial support. All numerical calculations were performed in Python (NumPy); the scripts reproducing every number are listed in Appendix A.

A Scripts

All scripts use NumPy only (`hs_figure.py` additionally uses matplotlib for the drawing). They are distributed with the paper in the folder `code/`.

`hs_flow.py`	closed-form EH flow with (X, Y), cubic (9), exponents, admissibility tests
`hs_checks.py`	closed forms against threshold-function quadrature; (X, Y) heat-kernel counting in schemes A and B; roots inserted in the full flow
`hs_scan.py`	Tables 2–5 and the checks quoted in the text; output in `results.txt`
`hs_model.py`	phenomenological model flow, reproduction of the first version; output in `results_model.txt`
`hs_figure.py`	Figure 1
`rre.py`, `rre_run50.py`	nine-regulator threshold functions and fixed-point search of the book (unchanged)

The core of the fixed-point search (Proposition 2.2) is:

```
import numpy as np
pi = np.pi
def B2(l):  u = 1-2*l; return -(5/u - 6/u**2)/(12*pi)
def fixed_points(X, Y):
    c = 14 - X
    out = []
    for u in np.roots([2*c, -(2*c + 54 - 3*Y), 118.0, -48.0]):
        if abs(u.imag) < 1e-9 and u.real > 0:
            u = u.real
```

```
            N = 4/u**2 - 2.5/u + c/6
            if N <= 0: continue
            g, l = 2*pi/N, (1-u)/2
            if 1 - g*B2(l) > 0:
                out.append((g, l))
    return out
# fixed_points(0, -6)  ->  [(2.7319, -0.3179)]    n_f = 3, two Proca
# fixed_points(1, -62) ->  [(3.2172, -4.3931)]    Standard Model
```

References

[1] S. Weinberg, Ultraviolet Divergences in Quantum Theories of Gravitation, in General Relativity: An Einstein Centenary Survey, eds. S. W. Hawking and W. Israel, Cambridge University Press (1979) 790–831.

[2] C. Wetterich, Exact Evolution Equation for the Effective Potential, Physics Letters B **301** (1993) 90–94.

[3] M. Reuter, Nonperturbative Evolution Equation for Quantum Gravity, Physical Review D **57** (1998) 971–985.

[4] A. Codello, R. Percacci, C. Rahmede, Investigating the Ultraviolet Properties of Gravity with a Wilsonian Renormalization Group Equation, Annals of Physics **324** (2009) 414–469.

[5] P. Donà, A. Eichhorn, R. Percacci, Matter matters in asymptotically safe quantum gravity, Physical Review D **89** (2014) 084035, arXiv:1311.2898.

[6] O. Lauscher, M. Reuter, Flow equation of quantum Einstein gravity in a higher-derivative truncation, Physical Review D **66** (2002) 025026, arXiv:hep-th/0205062.

[7] L. E. Pavesi, Quantum Distortion Gravity: Classical Foundations, Gauge Structure and the Einstein–Hilbert Flow with QDG-Like Matter, SSRN preprint (2026), `https://doi.org/10.2139/ssrn.7589303`.

[8] L. E. Pavesi, Quantum Distortion Gravity: One-Loop Beta Functions and the Absence of a Physical Fixed Point at $n_f = 3$, (2026) (earlier version of the companion note).

[9] L. E. Pavesi, Quantum Distortion Gravity: The UV Fixed Point Requires a Large Hidden Sector, (2026) (first version of the present paper).